

Review

Brain Protection in the Endo-Management of Proximal Aortic Aneurysms

Lydia Hanna ^{1,2,*} and Richard Gibbs ^{1,2}

¹ Department of Surgery and Cancer, Imperial College London, London W21NY, UK; r.gibbs@imperial.ac.uk

² Imperial Vascular Unit, Imperial College Healthcare NHS Trust, London W21NY, UK

* Correspondence: l.hanna@imperial.ac.uk

Received: 1 June 2020; Accepted: 22 June 2020; Published: 1 July 2020



Abstract: Neurological brain injury (NBI) remains the most feared complication following thoracic endovascular aortic repair (TEVAR), and can manifest as clinically overt stroke and/or more covert injury, detected only on explicit neuropsychological testing. Microembolic signals (MES) detected on transcranial Doppler (TCD) monitoring of the cerebral arteries during TEVAR and the high prevalence and incidence of new ischaemic infarcts on diffusion-weighted magnetic resonance imaging (DW-MRI) suggests procedure-related solid and gaseous cerebral microembolisation to be an important cause of NBI. Any intervention that can reduce the embolic burden during TEVAR may, therefore, help mitigate the risk of stroke and the covert impact of ischaemic infarcts to the function of the brain. This perspective article provides an understanding of the mechanism of stroke and reviews the available evidence regarding potential neuroprotective strategies that target high-risk procedural steps of TEVAR to reduce periprocedural cerebral embolisation.

Keywords: Thoracic aorta; stroke; covert stroke; DW-MRI infarcts; neurocognitive decline; neuroprotective adjuncts; cerebral embolic filter protection devices; carbon-dioxide flushing

1. Introduction

In recent years, the issue of neurological brain injury (NBI) following thoracic endovascular aortic repair (TEVAR) has become very relevant with increasing uptake of the procedure, and expansion to a younger ‘low-risk’ patient population. Despite significant improvements in most of the major complications and the shortened hospital stay that TEVAR affords in comparison to open surgical repair (OSR) [1], the stroke rate remains unchanged between the two modalities at 3–8% [1,2]. If anything, the introduction of new technology, particularly for total endovascular repair to treat the aortic arch, reveals a stroke rate that can be as high as 16% [3–5]. TEVAR associated stroke carries a poor prognosis, with a 30–50% in-hospital mortality [6].

In addition to clinical stroke, the widespread availability of advanced diffusion-weighted magnetic resonance imaging (DW-MRI) techniques has revealed that up to 81% of patients will have evidence of new cerebral infarcts, indicative of an ischaemic event, but without overt focal neurological deficits within 72 hrs of TEVAR (Figure 1) [7,8]. The clinical significance of this diffuse procedure-related brain damage remains to be fully elucidated in TEVAR, but may lead to persistent early neurologic deficit and functional losses on neuropsychological testing [7]. This perspective article aims to provide an overview of NBI following TEVAR, and reviews the evidence for potential contemporary neuroprotective adjuncts.

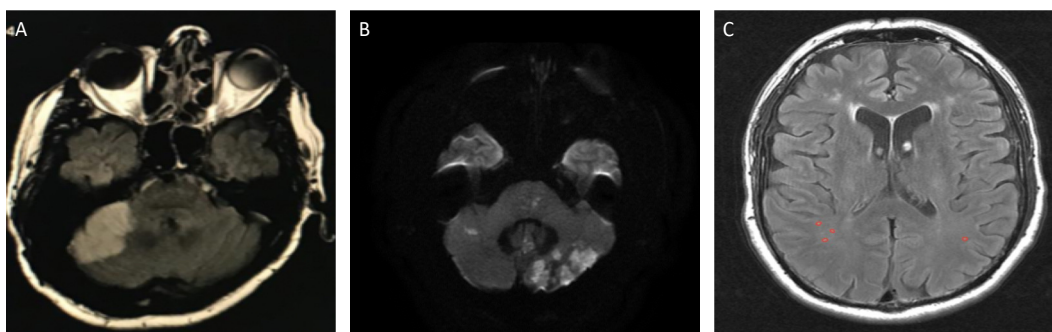


Figure 1. Diffusion-weighted magnetic resonance imaging showing: (A) Large infarct in right cerebellar hemisphere; (B) multiple infarcts in left cerebellar hemisphere; (C) multiple small (<3 mm) infarcts (red circles) in the posterior circulation.

2. The Spectrum of Neurological Brain Injury (NBI)

While overt clinical stroke is the most recognized neurological complication following TEVAR, there is increasing recognition that TEVAR and other transcatheter based cardiovascular interventions, such as transcatheter aortic valve implantation (TAVI), carotid artery stenting (CAS), as well as cardiac surgical procedures, result in a high incidence of ‘silent’ ischaemic cerebral infarcts (SCI) on DW-MRI [9–16]. The term ‘silent’ emphasises the absence of apparent focal neurological deficit, but is a misnomer for several reasons.

Firstly, patients are rarely systematically interrogated for neurological deficits in the postoperative period; cardiovascular studies that incorporate the routine neurological examination of patients by a neurologist have demonstrated a higher pick-up rate of neurological deficits than previous reports [17]. In addition, neurological examination provides objective assessment of only one aspect of brain function (motor and sensory). A complete evaluation of the functioning of the brain requires assessment of higher cognitive functions, such as memory, executive function, and language that can only be done through explicit neuropsychological testing. This is rarely undertaken in routine clinical practice. Any disturbances in cognition and behaviour in the post-operative period are often attributed to other causes, such as the effects of anaesthesia and other drugs, with no regard for a possible connection to embolic events within the brain.

Secondly, several longitudinal population-based studies have demonstrated significant associations between incident cerebral infarcts and a two to three-fold increased risk of future stroke, depression, and dementia. Participants with DW-MRI infarcts also display a steeper decline in cognitive function than those without infarcts [18,19]. More recently, a meta-analysis of large observational studies also confirmed these associations, and in particular, associated infarcts with a significant risk of death [20]. Cognitive function is known to be mediated by interconnected and complex neuronal circuitry of the brain and DW-MRI infarcts represent irreversible neuronal cell death in 98% of cases [21]. It is, therefore, plausible to assume that an infarct in any area of the brain has the potential to disrupt these connections and impact on higher functioning, akin to the pathophysiology of microinfarcts in Alzheimer’s disease [22].

Thirdly, increasing volumes of ‘subclinical’ procedure-related embolic infarcts have also been found to be significantly associated with postoperative cognitive dysfunction on explicit neuropsychological testing in patients undergoing cardiac and carotid revascularisation [23,24]. In the only study examining the impact of new DW-MRI infarcts, on cognitive function using a battery of well-validated neuropsychological testing after TEVAR, early neuropsychological decline was evident in 88% of patients [7].

The significance of these issues has been recognised, and in 2017, the Neurological Academic Research Consortium (NeuroARC) proposed standardized neurological endpoints for cardiovascular clinical trials. Procedural stroke is now defined as type 1, overt central nervous system (CNS) injury-acutely symptomatic brain or spinal cord injury, whereas the term type 2 covert CNS

injury is defined as acutely asymptomatic brain or spinal cord injury detected by neuroimaging. This classification underscores the increasing awareness that DW-MRI infarcts may not be completely free from clinical consequences [25].

3. Mechanism of Neurological Brain Injury

The mechanism of NBI in TEVAR is multifactorial and important to understand for the development of neuroprotective strategies. Patient and disease-specific risk factors for stroke following TEVAR include age, prior stroke, atheromatous disease of the aortic arch, as well as procedural aspects, such as proximal extent of repair and cerebral hypoperfusion from coverage of supra-aortic vessels and/or haemodynamic disturbance [6,26–30].

More than 90% of clinical stroke occurs within the first 24 hours of TEVAR. This temporal pattern, in addition to the focal and multi-focal appearance of ischaemic infarcts on postoperative brain MRI [6–8,27,30] as well as the detection of high-intensity microembolic signals (HITS/MES), which are indicative of microemboli passing through the cerebral circulation on transcranial Doppler (TCD) monitoring during TEVAR, suggests cerebral embolization to be the prevailing mechanism of stroke [7,31]. The total number of MES generated during TEVAR is a known significant predictor of subsequent transient ischaemic attack, stroke, and death ($p \leq 0.01$) [31], and postoperative cognitive decline ($p \leq 0.01$) [7].

TCD monitoring has identified several high-risk phases for cerebral microembolisation during TEVAR; wire and catheter manipulation, and device deployment generate the greatest number of MES [7,31,32]. TCD differentiation software has also allowed for the discrimination of MES as solid or gas based on the acoustic impedance and ultrasound reflectivity of embolic ‘material’ [32]; The greatest proportion of solid to gaseous MES appears to occur at wire and catheter manipulation. Conversely, more than 90% of the MES at device deployment have been found to be gaseous (Figure 2A) [32].

These findings are clinically translatable; the manipulation of endovascular instruments and deployment of sizeable stent-grafts in a diseased atherosclerotic aortic arch as well as the prothrombotic tendency of wires and catheters may lead to dislodgement of atheromatous debris, arterial wall, fresh and organized thrombus. Indeed, several studies have identified severe atheromatous disease of the aortic arch to be a significant risk factor for stroke and new DW-MRI infarcts (Figure 2B) [6,26,28,32]. Furthermore, several benchtop studies have demonstrated that all commercially available TEVAR devices release significant amounts of ‘air’ bubbles, which are presumably retained from the manufacturing processes, despite flushing with heparinized-saline to remove air from within the device. Benchtop studies clearly demonstrate that air bubbles distribute to the supra-aortic vessels upon deployment. Interestingly, and perhaps unsurprisingly, different amounts of gaseous bubbles are released from stent-grafts of the same manufacturer, and between differing manufacturing companies, with unsheathed devices releasing the least amount of air [33–35].

The proximity of endovascular instrumentation to arch vessels, vortical and helical flow patterns, as well as temporary loss of antegrade flow with a large device in the arch, and reduced clearance of emboli from periprocedural cerebral hypoperfusion may all facilitate the passage of solid and gaseous microemboli into the cerebral circulation [33]. Once in the cerebral vasculature, microemboli may become trapped if the size of the embolus is greater to the vessel diameter, leading to the mechanical obstruction of blood flow, or they may incite endothelial damage and an inflammatory response as they redistribute throughout the circulation. The final insult is ischaemia and neuronal cell death in downstream tissue [36,37].

While solid emboli are thought to be more dangerous for the brain than gaseous emboli because of the transient nature of the latter under the force of pulsatile blood and rapid diffusion, data from animal models of cerebral air embolization, and following ‘gaseous generating’ intravascular procedures such as cardiac angiography have demonstrated radiological evidence of cerebral infarction following introduction of air into the circulation [38–41].

In TEVAR, positive correlations between solid MES and new DW-MRI infarcts ($r_s = 0.928; p = 0.01$) as well as gaseous MES and new DW-MRI infarcts ($r_s = 0.912; p = 0.01$) clearly demonstrate the harmful effects of both solid and gaseous emboli to the brain [32]. The significant association between number of solid MES and increased surface area of DW-MRI infarcts (but not number of DW-MRI infarcts), and between number of gaseous MES and increasing number of DW-MRI infarcts (but not surface area of DW-MRI infarcts), especially those <3 mm in diameter, suggests that solid emboli may account for more focal destruction of cerebral tissue, whereas gaseous emboli account for the more diffuse pattern of injury (Figure 2C,D) [32].

While a potential hypothesis from these findings could be that solid emboli are more likely to lead to focal neurological deficit, with gaseous emboli causing a decline in global brain dysfunction, the clinical consequences of solid and/or gaseous emboli are likely to be dependent on the location of the infarct/s—A small infarct in the internal capsule may lead to devastating hemiparesis or hemiplegia, yet a similar infarct at this location, or elsewhere in the brain may be sufficient to disrupt complex interconnected cognitive neuronal networks [22].

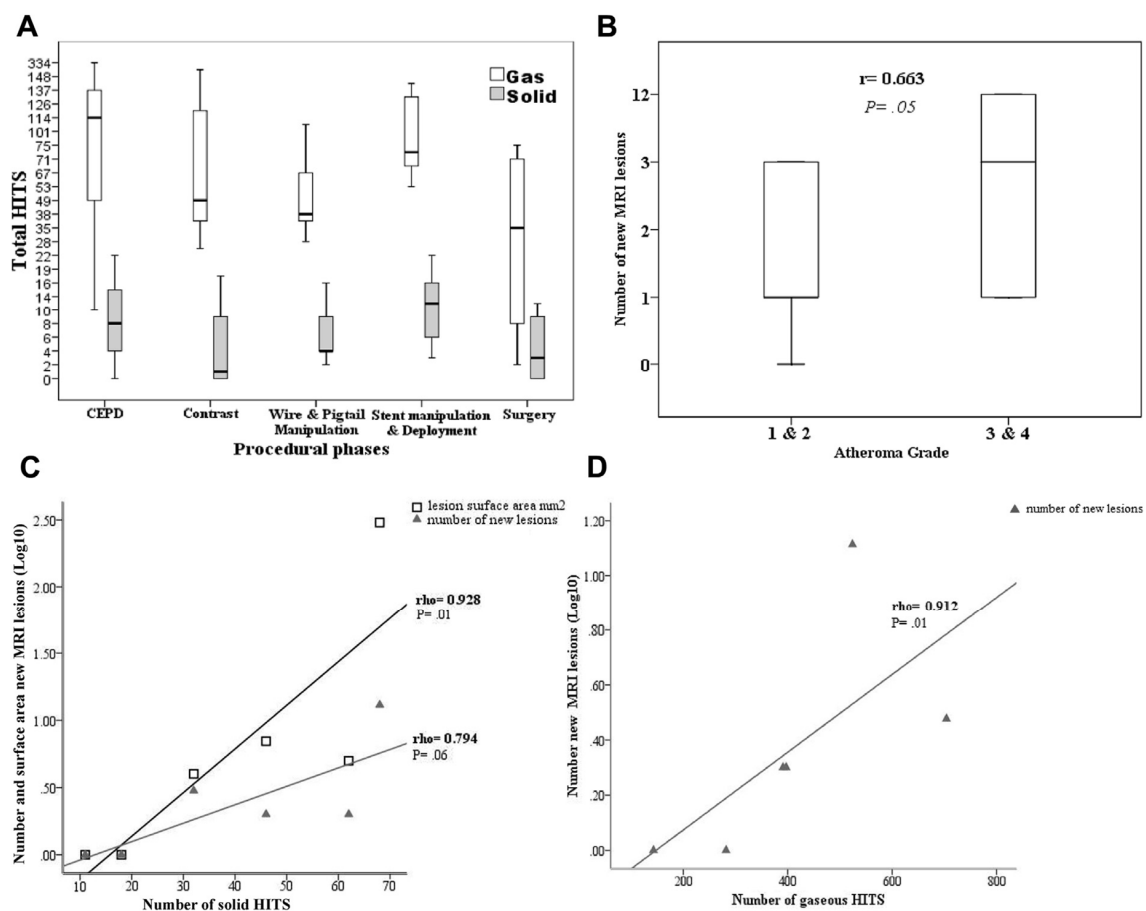


Figure 2. (A) Procedural solid and gaseous high-intensity transient signals (HITS). (B) Pearson’s correlation between new magnetic resonance imaging (MRI) lesions ≥ 14.3 mm in diameter and grade of atheroma on the aortic arch. (C) Spearman’s rank correlation between number of solid HITSs and number and surface area of new MRI lesions. (D) Spearman’s rank correlation between the number of gaseous HITSs and number of new MRI lesions [32].

4. Neuroprotective Strategies against Solid Cerebral Embolisation

4.1. Cerebral Embolic Protection Devices (CEPDs)

CEPDs are dedicated filters designed to deflect or capture emboli ‘en-route’ to the brain as adjunctive therapy during cardiovascular transcatheter based procedures where there is a significant periprocedural embolic risk, such as in CAS and TAVI [9–16]. CEPDs are inserted prior to commencement of the transcatheter based procedure, and are retrieved on completion of the procedure. CEPDs differ in structure (frame vs. cone), access (radial/brachial vs. femoral), filter pore and sheath size, mechanism of protection (deflection vs. filter and capture), location (across the arch or into supra-aortic vessels), and which supra-aortic vessels are afforded protection (Table 1).

Table 1. Commercially available cerebral embolic protection devices.

	Embrella (Edwards Lifesciences; Irvine, CA, United States)	TriGuard (Keystone Heart Ltd., Herzliya, Israel)	SENTINEL™ (Boston Scientific, MA, United States)
Structure	Two polyurethane membrane/mesh (pore size 100um) mounted on a nitinol frame	Nitinol frame and polymeric membrane/mesh (pore size 115 × 145 um)	Two cone shaped mesh filters (pore size 140 um, proximal filter 15 mm in size, distal filter 10 mm in size) connected by an articulating catheter
Placement	Aortic Arch	Aortic Arch	Directly into brachiocephalic (proximal filter) and left common carotid artery (distal filter)
Access and Sheath Size	Radial/ulnar/brachial 6F	Femoral 9F	Radial/brachial 6F
Embolic protection method	Deflection	Deflection	Filter and capture
Supra-aortic vessels protected	Brachiocephalic and left common carotid arteries	Brachiocephalic, left common carotid and left subclavian arteries	Brachiocephalic and left common carotid arteries
Vascular territory protection	Anterior circulation	Anterior and posterior circulation	Anterior circulation

There is a paucity of data on the use of CEPDS in TEVAR; however, useful insights can be gained from the use of CEPDs in TAVI, an endovascular technique with procedural similarities to TEVAR. A number of randomised and large prospective studies using clinical and radiological end-points in patients undergoing TAVI largely demonstrate a reduction in periprocedural stroke rate as well as a reduction in the number and volume of new DW-MRI infarcts when compared to patients who did not receive CEPD [10–15]. The SENTINEL™ trial further demonstrated a significant correlation between new lesion number and volume, and neurocognitive decline [15]. Histological confirmation of the high embolic load (majority of debris 150–500 mm in diameter) captured by CEPDs further supports the hypothesis that CEPDs have the potential to mitigate periprocedural embolic risk from TAVI (Table 2) [10,11,15].

The efficacy of CEPD use in TAVI, as indicated in these studies, in addition to the comparable cardioembolic risk profile, and overt and covert neurological event rate between TEVAR and TAVI suggests that CEPDs could also potentially confer neuroprotection in patients undergoing TEVAR. However, unlike TAVI, TEVAR is dependent on a landing zone within or close to the arch. This limits the applicability of many of the devices used in TAVI for use in standard TEVAR workflow. In particular, CEPDs that protect the supra-aortic trunks by sitting across the arch may interfere with fixation and sealing of the TEVAR stent-graft (Embrella and TriGuard).

Table 2. Evidence base for cerebral embolic protection devices.

	Embrella (Edwards Lifesciences; Irvine, California, United States)	TriGuard (Keystone Heart Ltd., Herzliya, Israel)	SENTINEL™ (Boston Scientific, MA, United States)
Pivotal study/s	PROTAVI-C	DEFLECT III	CLEAN-TAVI ¹ MISTRAL-C ¹ SENTINEL ¹ CSI-Ulm-TAVR ²
Methods	Prospective, non-randomised	RCT	1.RCT 2.Prospective non-randomised
Patients (CEPD vs. controls)	41 vs. 11	46 vs. 39	CLEAN-TAVI: 50 vs. 50 MISTRAL-C: 32 vs. 33 SENTINEL: 244 vs. 119 CSI-Ulm-TAVR: 802
Results	<p><u>Stroke/TIA</u> 7.3% CEPD vs. control 0% ($p > 0.05$)</p> <p><u>DW-MRI:</u> Non-significant increase in DW-MRI infarcts in CEPD group (8vs.4, $p = 0.41$) Significantly lower DW-MRI infarct volumes (40% smaller, $p = 0.003$) in CEPD group</p> <p><u>Neurocognitive</u> Mild significant improvement at 30 days compared with baseline in CEPD group ($p < 0.001$) vs. no difference in control group over time ($p = 0.678$)</p>	<p><u>Stroke/TIA</u> 2.2% CEPD vs. 5.1 control ($p = 0.46$) 3.1% worsening NIHSS score from baseline in CEPD vs. 15.4% control ($p = 0.16$)</p> <p><u>DW-MRI:</u> Greater freedom from DW-MRI infarct in CEPD (21.2 vs. 11.5%), -44% reduction of median DW-MRI infarct volume ($p = 0.07$)</p> <p><u>Neurocognitive</u> At discharge and at 30 days, fewer TriGuard patients in both the ITT and PT populations had a worsening in MoCA scores Mean MoCA score improved from baseline to discharge and 30 days in the TriGuard group; in the control group, the mean score declined from baseline to discharge and rebounded to approximately baseline levels at 30 days</p>	<p><u>Stroke/TIA</u> CLEAN-TAVI: 5% CEPD vs. control 5% MISTRAL-C 0% CEPD vs. control 7% SENTINEL: 5.6% vs. 9.1%; $p = 0.25$) CSI-Ulm-TAVR: 1.4% vs. 4.2% ($p = 0.03$)</p> <p><u>DW-MRI</u> CLEAN-TAVI: significantly lower number and volume of DW-MRI in CEPD group ($p < 0.001$) MISTRAL-C: Greater freedom from DW-MRI infarct in CEPD (27% vs. 13%), lower number and volume of DW-MRI infarcts SENTINEL: significant reductions in DW-MRI volume in both protected and all territories in the CEPD group vs. controls ($p = 0.025$ and $p = 0.050$ for protected and all territories, respectively. CSI-Ulm-TAVR: Neurocognitive: CLEAN-TAVI: 50% vs. 72.2% overall worsening early MoCA scores MISTRAL-C: 4% vs. 27% cognitive deterioration ($p = 0.017$) SENTINEL: Significant correlation between change in neurocognitive scores from baseline to 30-day follow-up with median DW-MRI lesion volume in protected territories ($p = 0.0109$) and unprotected territories ($p = 0.003$)</p>

CEPD, cerebral embolic protection device; DW-MRI, diffusion-weighted imaging; ITT, intention to treat; PT, per protocol; NIHSS, National Institute of Health Stroke Scale; MoCA, Montreal Cognitive Assessment.

The most relevant CEPD to TEVAR is the SENTINEL™ dual-filter system. This involves the percutaneous insertion of a proximal and distal filter directly into the brachiocephalic and left common carotid artery. Three very small feasibility and safety studies of the Sentinel™ CEPD in TEVAR are reported in the literature (total of 17 patients) [16,32,42]. The most comprehensive study is that by Grover et al. [28] who demonstrate that out of the 10 patients undergoing TEVAR with the Sentinel™ CEPD, there was a 95% debris capture rate of acute thrombus, arterial wall and foreign material with a median total number and 937 captured particles (interquartile range 146–1687) and median surface area of 2.66 mm² (interquartile range, 0.08–9.18 mm²). Furthermore, there was no case of stroke and only 23 new infarcts with a median surface area of 6 mm² were detected with DW-MRI in the CEPD group in comparison to the documented 13% stroke rate and 120 new infarcts with a median surface area of 16 mm² in patients undergoing TEVAR without protection, as reported by Perera et al. [7].

Significant associations between subtle neurological injury in the form of cognitive decline, and ischaemic burden (multiple DW-MRI infarcts or single infarcts greater than 1cm³) in carotid and cardiac revascularisation procedures have been described [23,24]. The reduction in the number and size of DW-MRI infarcts with CEPD protection, therefore, has the potential to translate to improved cognitive

outcomes in patients undergoing TEVAR. While these results are promising, further evaluation in large studies is necessary in order to support routine clinical use.

The major drawback of the Sentinel™ CEPD for use in TEVAR (and TAVI) is incomplete brain protection. The left vertebral artery, which provides up to 20% of total brain perfusion, remains unprotected by the current generation of Sentinel™ CEPD, thereby allowing passage of periprocedural debris to the brain through this vessel. Unsurprisingly, Grover et al. report that the majority of new infarcts (65%) in patients undergoing TEVAR with the Sentinel™ CEPD were located in the hindbrain territory supplied by the left subclavian/vertebral artery (Figure 3) [32]. Similarly, three randomised trials in TAVI with CEPD (CLEAN-TAVI, MISTRAL-C, and SENTINEL™) have also shown a lower reduction in lesion volume to the entire brain, in comparison to the protected areas. The unprotected left vertebral artery in all of these studies may account for this finding

To this end, Van Gils et al. have recently evaluated the concept of complete brain protection with CEPDs by deploying a single filter, the Wirion (Allium Medical, Inc., Caesarea, Israel) into the left vertebral artery, in addition to Sentinel™ CEPD placement into the brachiocephalic and left common carotid arteries in 11 patients undergoing TAVI (Figure 4). While the small sample size prevents assessment of clinical benefit, the study did demonstrate comparable amount and size of embolic debris in the left vertebral filter to the Sentinel filters, which would have otherwise presumably reached the brain [43].

A further limitation of the Sentinel™ CEPD in TEVAR is the inability to deploy it with TEVAR in zone 0 and 1 due to interference with deployment of both filters relative to the stent-graft, as well as filter retrieval, that may result in displacement of the stent-graft or entrapment of the CEPD. Shimamura et al. describe their experience with selective deployment of three different single filters (Parachute (Tri-Med), Filtrap (Nipro), and FilterWire EZ (Boston Scientific Corporation)) in the supra-aortic vessels with routine placement of an occlusion balloon catheter for the left subclavian artery following arch debranching procedures, but prior to TEVAR stent-graft deployment, in zone 0 and 1 in a complex group of 17 patients. The authors conclude that the use of single filters may prevent stroke during endovascular arch repair [44]. However, while TEVAR is performed under CEPD protection, the debranching procedures required to revascularise the brachiocephalic and left common carotid arteries at these landing zones is unprotected and could also be a further source for embolic stroke. [10,11,15].

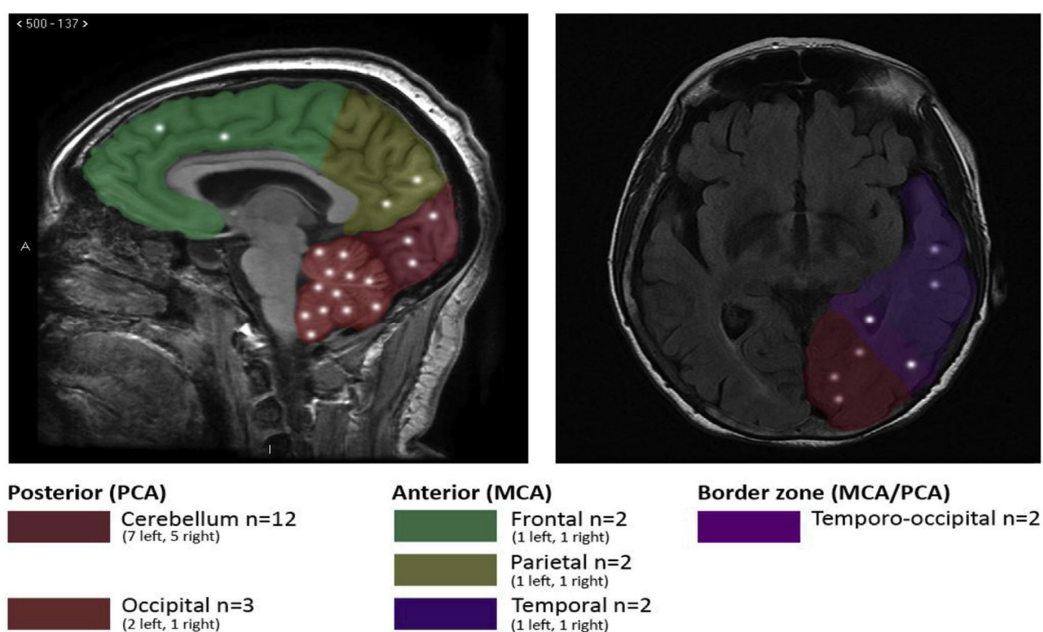


Figure 3. Vascular distribution of diffusion-weighted magnetic resonance imaging infarcts. MCA, middle cerebral artery; PCA, posterior cerebral artery [32].

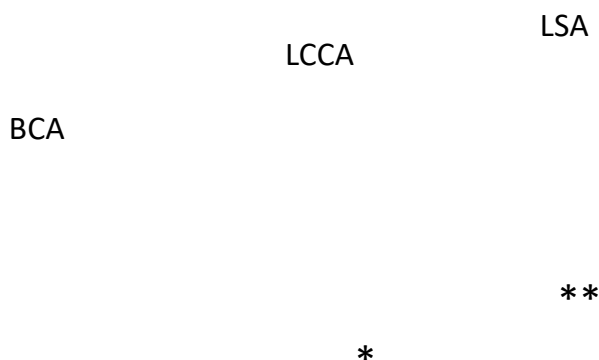


Figure 4. Pictorial representation of the dual-filter SentinelTM CEPD(*) with filters in the brachiocephalic artery (BCA) and left common carotid artery (LCCA), and a filter (**) in the left subclavian artery (LSA) to provide complete protection to all cerebrovascular territories.

4.2. Carotid Clamping and Flow Reversal

Supra-aortic vessel clamping is an alternative method of embolic protection and has been utilised in CAS to prevent cerebral embolisation into the internal carotid artery (ICA) [45]. Masada et al. describe their outcomes with a similar technique in TEVAR whereby native forward blood flow from the left common carotid artery and the left subclavian artery for zone 1 cases and from the left subclavian artery for zone 2 cases is arrested with clips and occlusion balloons applied to these vessels before delivery and deployment of stent-grafts. The authors attribute the 21% rate of infarction (24 new infarcts) in this TEVAR cohort to this technique [46].

The concept of flow reversal to divert blood (and emboli) away from the cerebral vessels during CAS may also prove to be a promising strategy during interventions in the aortic arch. Ribo et al. document that TCD monitoring did not detect any air/solid microemboli during stent deployment or angioplasty in 65 patients undergoing CAS with flow reversal [47]. Furthermore, a recent meta-analysis of single-arm and comparative studies demonstrated a pooled stroke rate of 0–4% during CAS with flow reversal [48].

Both of these techniques, however, require surgical exposure of the supra-aortic vessels that may not be necessary for all TEVAR cases. Clamping of the supra-aortic vessels and flow reversal also risk cerebral hypoperfusion, while clamp release may itself lead to cerebral embolisation, all of which risk neurological deficit.

4.3. Robotic Navigation

The maximum proportion of solid to gaseous emboli occur during wire and pigtail manipulation [32]. The use of robotic catheters in the arch is thought to increase precise manoeuvrability and stability of endovascular instruments in the arch. This technology may therefore reduce unnecessary catheter movements and contact with an atherosclerotic vessel wall that risks dislodgement of particulate matter. In a simulation study, Rippel et al. demonstrate a significant reduction in vessel wall contact (wall-hits) with robotic catheter technology compared to manual techniques in TAVI (median wall-hits: 1 (0–5) vs. 6 (2–22), $p < 0.01$) [49]. Perera et al. translate these findings in-vivo in patients undergoing TEVAR whereby robotic navigation significantly reduced TCD-detected cerebral embolisation of particulate matter during catheter placement in the arch in comparison to manual techniques (median TCD-HITS: 0(0–1) vs. 2(1–5), $p < 0.01$) [50]. The potential to reduce overall periprocedural embolic load with this technology may also mitigate ischaemic damage to the brain, perioperative and future stroke as well as neurocognitive impairment.

5. Neuroprotective Strategies against Gaseous Cerebral Embolisation

5.1. TEVAR Delivery System Flushing Techniques

The increasing awareness that TEVAR devices retain significant amounts of air from the manufacturing processes despite flushing with heparinised-saline according to instructions for use (IFU), and the potential for air bubbles released during deployment to embolise to the brain and incite ischaemic damage, highlights the need for improved techniques with which to prepare both sheathed and unsheathed devices prior to introduction into a patient.

The unique properties of carbon-dioxide (denser and 25× more soluble to air) in displacing air to prevent cerebral air microembolism and improve neurological outcome has been widely reported in patients undergoing open heart surgery [51–53]. This has translated into the practice of ‘CO₂ flushing’ of TEVAR devices to replace air within the spaces of the delivery system and stent-graft with a less harmful gas [29]. Kolbel et al. report a 3% stroke rate in 36 patients [54] while Hanna et al. report an 7.5% stroke rate in 53 patients undergoing TEVAR with CO₂ flushing [55]. Notably, this latter study did demonstrate that only 39% of patients had evidence of new DW-MRI infarcts which contrasts to the 63–81% rate of infarction reported in other studies [7,8]. The neurocognitive impact of the reduced embolic burden requires further study. Other device specific de-airing techniques have also been described including the use of ‘blood flushing’, addition of flushing side ports, and liquid perfluorocarbons, however, there is insufficient clinical data to support their use at this time [56,57].

5.2. Gaseous Filter Devices

The overwhelming number of total gaseous MES compared to solid MES (391 gaseous MES vs. 32 solid MES), and during all procedural steps of TEVAR (Figure 2A) [28] places greater significance on cerebral air microembolisation as a major source of NBI than previously envisaged. This is keeping with open cardiac surgery whereby the use of oxygenators can lead to cerebral microembolisation and neurocognitive decline [58]. The use of a dynamic bubble trap (HPmedica, Augsburg, Germany) designed to reduce gaseous embolisation has been found to reduce TCD MES with improved cognitive function three months following coronary artery bypass, and the TriGuard 3 CEPD reduced cerebral embolization of particulate and air bubbles under simulated conditions [59]. In the future, technological developments could focus on the design of supra-aortic vessel filters that prevent the passage of both solid and gaseous microemboli during TEVAR.

6. Conclusions

The importance of TEVAR as a therapeutic option for older, comorbid patients with thoracic aortic disease and the inherent risk of stroke and cognitive decline in this population, as well the expansion of TEVAR to a younger and ‘lower-risk’ cohort of patients demands the application of strategies that can mitigate all forms of procedure-related brain injury including ischaemic cerebral infarcts. At this current time, there are no TEVAR-specific neuroprotective systems/adjuncts against neurological brain injury. CEPDs and meticulous preparation of TEVAR delivery systems, which may include the use of carbon-dioxide flushing to prevent periprocedural cerebral embolisation of particulate matter and air offer promising neuroprotective solutions but further clinical studies are required to show direct correlation between these practices and improved clinical and radiological outcomes.

Author Contributions: Conceptualisation, L.H. and R.G.; writing-original draft preparation, L.H.; writing-review and editing, R.G.; supervision; R.G. All authors have read and agreed to the published version of the manuscript.

Funding: This research was funded by Imperial Healthcare Charity, Grant number 181910.

Conflicts of Interest: The authors declare no conflict of interest.

References

1. Cheng, D.; Martin, J.; Shennib, H.; Dunning, J.; Muneretto, C.; Schueler, S.; Von Segesser, L.; Sergeant, P.; Turina, M. Endovascular aortic repair versus open surgical repair for descending thoracic aortic disease: A systematic review and meta-analysis of comparative studies. *J. Am. Coll. Cardiol.* **2010**, *55*, 986–1001. [[CrossRef](#)] [[PubMed](#)]
2. Harky, A.; Chan, J.S.; Wong, C.H.; Bashir, M. Open versus endovascular repair of descending thoracic aortic aneurysm disease: A systematic review and meta-analysis. *Ann. Vasc. Surg.* **2019**, *54*, 304–315. [[CrossRef](#)] [[PubMed](#)]
3. Haulon, S.; Greenberg, R.K.; Spear, R.; Eagleton, M.; Abraham, C.; Lioupis, C.; Verhoeven, E.; Ivancev, K.; Kölbel, T.; Stanley, B. Global experience with an inner branched arch endograft. *J. Thorac. Cardiovasc. Surg.* **2014**, *148*, 1709–1716. [[CrossRef](#)]
4. Ferrer, C.; Coscarella, C.; Cao, P. Endovascular repair of aortic arch disease with double inner branched thoracic stent graft: The Bolton perspective. *J. Cardiol. Surg.* **2018**, *59*, 547–553.
5. Tsilimparis, N.; Debus, E.S.; von Kodolitsch, Y.; Wipper, S.; Rohlfes, F.; Detter, C.; Roeder, B.; Kölbel, T. Branched versus fenestrated endografts for endovascular repair of aortic arch lesions. *J. Vasc. Surg.* **2016**, *64*, 592–599. [[CrossRef](#)]
6. Gutsche, J.T.; Cheung, A.T.; McGarvey, M.L.; Moser, W.G.; Szeto, W.; Carpenter, J.P.; Fairman, R.M.; Pochettino, A.; Bavaria, J.E. Risk factors for perioperative stroke after thoracic endovascular aortic repair. *Ann. Thorac. Surg.* **2007**, *84*, 1195–1200. [[CrossRef](#)]
7. Perera, A.H.; Rudarakanchana, N.; Monzon, L.; Bicknell, C.D.; Modarai, B.; Kirimi, O.; Athanasiou, T.; Hamady, M.; Gibbs, R.G. Cerebral embolization, silent cerebral infarction and neurocognitive decline after thoracic endovascular aortic repair. *Br. J. Surg.* **2018**, *105*, 366–378. [[CrossRef](#)]
8. Kahlert, P.; Eggebrecht, H.; Jánosi, R.A.; Hildebrandt, H.A.; Plicht, B.; Tsagakis, K.; Moenninghoff, C.; Nensa, F.; Mummel, P.; Heusch, G.; et al. Silent cerebral ischemia after thoracic endovascular aortic repair: A neuroimaging study. *Ann. Thorac. Surg.* **2014**, *98*, 53–58. [[CrossRef](#)]
9. Gray, W.A.; Mehta, M.; Alani, F.; Kasirajan, K.; Begg, R.J.; Bacharach, J.M.; Soukas, P.A. EMBOLDEN Clinical Study Investigators. Use of a novel embolic filter in carotid artery stenting: 30-Day results from the EMBOLDEN Clinical Study. *Catheter. CardioVasc. Inter.* **2018**, *92*, 1128–1135. [[CrossRef](#)]
10. Haussig, S.; Mangner, N.; Dwyer, M.G.; Lehmkuhl, L.; Lück, C.; Woite, F.; Holzhey, D.M.; Mohr, F.W.; Gutberlet, M.; Zivadinov, R.; et al. Effect of a cerebral protection device on brain lesions following transcatheter aortic valve implantation in patients with severe aortic stenosis: The CLEAN-TAVI randomized clinical trial. *JAMA* **2016**, *316*, 592–601. [[CrossRef](#)]
11. Van Mieghem, N.M.; van Gils, L.; Ahmad, H.; Van Kesteren, F.; Van Der Werf, H.W.; Brueren, G.; Storm, M.; Lenzen, M.; Daemen, J.; van den Heuvel, A.F.; et al. Filter-based cerebral embolic protection with transcatheter aortic valve implantation: The randomised MISTRAL-C trial. *EuroIntervention* **2016**, *12*, 499–507. [[CrossRef](#)]
12. Lansky, A.J.; Schofer, J.; Tchetché, D.; Stella, P.; Pietras, C.G.; Parise, H.; Abrams, K.; Forrest, J.K.; Cleman, M.; Reinhoehl, J.; et al. A prospective randomized evaluation of the TriGuard™ HDH embolic DEFLECTION device during transcatheter aortic valve implantation: Results from the DEFLECT III trial. *Eur. Heart. J.* **2015**, *36*, 2070–2078. [[CrossRef](#)] [[PubMed](#)]
13. Rodés-Cabau, J.; Kahlert, P.; Neumann, F.J.; Schymik, G.; Webb, J.G.; Amarenco, P.; Brott, T.; Garami, Z.; Gerosa, G.; Lefèvre, T.; et al. Feasibility and exploratory efficacy evaluation of the Embrella Embolic Deflector system for the prevention of cerebral emboli in patients undergoing transcatheter aortic valve replacement: The PROTAVI-C pilot study. *JACC. Cardiovasc. Interv.* **2014**, *7*, 1146–1155. [[CrossRef](#)] [[PubMed](#)]
14. Wöhrle, J. Coronary and Structural Interventions Ulm Transcatheter Aortic Valve Replacement (CSI-Ulm-TAVR) University of Ulm. 2017. Available online: <https://clinicaltrials.gov/ct2/show/NCT02162069> (accessed on 28 May 2020).
15. Kapadia, S.R.; Kodali, S.; Makkar, R.; Mehran, R.; Lazar, R.M.; Zivadinov, R.; Dwyer, M.G.; Jilaihawi, H.; Virmani, R.; Anwaruddin, S.; et al. Protection against cerebral embolism during transcatheter aortic valve replacement. *J. Am. Coll. Cardiol.* **2017**, *69*, 367–377. [[CrossRef](#)] [[PubMed](#)]
16. Jánosi, R.A. Cerebral Protection against Embolization during Thoracic Endovascular Aortic Repair. *LINC*. 2016. Available online: http://claretmedical.com/pdf/studies/LINC_2016_Claret_Janosi_TEVAR.pdf (accessed on 28 March 2020).

17. Messé, S.R.; Acker, M.A.; Kasner, S.E.; Fanning, M.; Giovannetti, T.; Ratcliffe, S.J.; Bilello, M.; Szeto, W.Y.; Bavaria, J.E.; Hargrove III, W.C.; et al. Stroke after aortic valve surgery: Results from a prospective cohort. *Circulation* **2013**, *129*, 2253–2261. [[CrossRef](#)]
18. Cees De Groot, J.; De Leeuw, F.E.; Oudkerk, M.; Van Gijn, J.; Hofman, A.; Jolles, J.; Breteler, M.M. Cerebral white matter lesions and cognitive function: The Rotterdam Scan Study. *Ann. Neurol.* **2000**, *47*, 145–151. [[CrossRef](#)]
19. Forsberg, L.; Sigurdsson, S.; Fredriksson, J.; Egilsdottir, A.; Oskarsdottir, B.; Kjartansson, O.; van Buchem, M.A.; Launer, L.J.; Gudnason, V.; Zijdenbos, A. The AGES-Reykjavik study atlases: Non-linear multi-spectral template and atlases for studies of the ageing brain. *Med. Image. Anal.* **2017**, *39*, 133–144. [[CrossRef](#)]
20. Debette, S.; Schilling, S.; Duperron, M.G.; Larsson, S.C.; Markus, H.S. Clinical significance of magnetic resonance imaging markers of vascular brain injury: A systematic review and meta-analysis. *JAMA. Neurol.* **2019**, *76*, 81–94. [[CrossRef](#)]
21. Li, F.; Liu, K.F.; Silva, M.D.; Omae, T.; Sotak, C.H.; Fenstermacher, J.D.; Fisher, M.; Hsu, C.Y.; Lin, W. Transient and permanent resolution of ischemic lesions on diffusion-weighted imaging after brief periods of focal ischemia in rats: Correlation with histopathology. *Stroke* **2000**, *31*, 946–954. [[CrossRef](#)]
22. Suter, O.C.; Sunthorn, T.; Kraftsik, R.; Straubel, J.; Darekar, P.; Khalili, K.; Miklossy, J. Cerebral hypoperfusion generates cortical watershed microinfarcts in Alzheimer disease. *Stroke* **2002**, *33*, 1986–1992. [[CrossRef](#)]
23. Zhou, W.; Baughman, B.D.; Soman, S.; Wintermark, M.; Lazzeroni, L.C.; Hitchner, E.; Bhat, J.; Rosen, A. Volume of subclinical embolic infarct correlates to long-term cognitive changes after carotid revascularization. *J. Vasc. Surg.* **2017**, *65*, 686–694. [[CrossRef](#)]
24. Barber, P.A.; Hach, S.; Tippett, L.J.; Ross, L.; Merry, A.F.; Milsom, P. Cerebral ischemic lesions on diffusion-weighted imaging are associated with neurocognitive decline after cardiac surgery. *Stroke* **2008**, *39*, 1427–1433. [[CrossRef](#)] [[PubMed](#)]
25. Lansky, A.J.; Messé, S.R.; Brickman, A.M.; Dwyer, M.; van der Worp, H.B.; Lazar, R.M.; Pietras, C.G.; Abrams, K.J.; McFadden, E.; Petersen, N.H.; et al. Proposed standardized neurological endpoints for cardiovascular clinical trials: An academic research consortium initiative. *J. Am. Coll. Cardiol.* **2017**, *69*, 679–691. [[CrossRef](#)] [[PubMed](#)]
26. Kotelis, D.; Bischoff, M.S.; Jobst, B.; von Tengg-Kobligk, H.; Hinz, U.; Geisbüsch, P.; Böckler, D. Morphological risk factors of stroke during thoracic endovascular aortic repair. *Langenbecks. Archs. Surg.* **2012**, *397*, 1267–1273. [[CrossRef](#)] [[PubMed](#)]
27. Melissano, G.; Tshomba, Y.; Bertoglio, L.; Rinaldi, E.; Chiesa, R. Analysis of stroke after TEVAR involving the aortic arch. *Eur. J. Vasc. Endovasc. Surg.* **2012**, *43*, 269–275. [[CrossRef](#)]
28. Feezor, R.J.; Martin, T.D.; Hess, P.J.; Klodell, C.T.; Beaver, T.M.; Huber, T.S.; Seeger, J.M.; Lee, W.A. Risk factors for perioperative stroke during thoracic endovascular aortic repairs (TEVAR). *J. Endovasc. Ther.* **2007**, *14*, 568–573. [[CrossRef](#)] [[PubMed](#)]
29. Chung, J.; Kasirajan, K.; Veeraswamy, R.K.; Dodson, T.F.; Salam, A.A.; Chaikof, E.L.; Corriere, M.A. Left subclavian artery coverage during thoracic endovascular aortic repair and risk of perioperative stroke or death. *J. Vasc. Surg.* **2011**, *54*, 979–984. [[CrossRef](#)]
30. Ullery, B.W.; McGarvey, M.; Cheung, A.T.; Fairman, R.M.; Jackson, B.M.; Woo, E.Y.; Desai, N.D.; Wang, G.J. Vascular distribution of stroke and its relationship to perioperative mortality and neurologic outcome after thoracic endovascular aortic repair. *J. Vasc. Surg.* **2012**, *56*, 1510–1517. [[CrossRef](#)]
31. Bismuth, J.; Garami, Z.; Anaya-Ayala, J.E.; Naoum, J.J.; El Sayed, H.F.; Peden, E.K.; Lumsden, A.B.; Davies, M.G. Transcranial Doppler findings during thoracic endovascular aortic repair. *J. Vasc. Surg.* **2011**, *54*, 364–369. [[CrossRef](#)]
32. Grover, G.; Perera, A.H.; Hamady, M.; Rudarakanchana, N.; Barras, C.D.; Singh, A.; Davies, A.H.; Gibbs, R. Cerebral embolic protection in thoracic endovascular aortic repair. *J. Vasc. Surg.* **2018**, *68*, 1656–1666. [[CrossRef](#)]
33. Inci, K.; Koutouzi, G.; Chernoray, V.; Jeppsson, A.; Nilsson, H.; Falkenberg, M. Air bubbles are released by thoracic endograft deployment: An in vitro experimental study. *SAGE. Open. Med.* **2016**, *4*, 20. [[CrossRef](#)] [[PubMed](#)]

34. Rohlffs, F.; Tsilimparis, N.; Saleptsis, V.; Diener, H.; Debus, E.S.; Kölbl, T. Air embolism during TEVAR: Carbon dioxide flushing decreases the amount of gas released from thoracic stent-grafts during deployment. *J. Endovasc. Ther.* **2017**, *24*, 84–88. [[CrossRef](#)] [[PubMed](#)]
35. Gagnon, J.; Tittley, J.; Misskey, J.D. IP063. Analysis and Quantification of Retained Air in Thoracic Aortic Endografts. *J. Vasc. Surg.* **2017**, *65*, 73S. [[CrossRef](#)]
36. Gorman, D.F.; Browning, D.M. Cerebral vasoreactivity and arterial gas embolism. *Undersea. Biomed. Res.* **1986**, *13*, 317–335. [[PubMed](#)]
37. Kudo, M.O.; Aoyama, A.K.; Ichimori, S.H.; Fukunaga, N. An animal model of cerebral infarction. Homologous blood clot emboli in rats. *Stroke* **1982**, *13*, 505–508. [[CrossRef](#)]
38. Gerriets, T.; Walberer, M.; Nedelmann, M.; Doenges, S.; Ritschel, N.; Bachmann, G.; Stolz, E.; Kaps, M.; Urbanek, S.; Urbanek, P.; et al. A rat model for cerebral air microembolisation. *J. Neurosci. Methods.* **2010**, *190*, 10–13. [[CrossRef](#)]
39. Lund, C.; Nes, R.B.; Ugelstad, T.P.; Due-Tønnessen, P.; Andersen, R.; Hol, P.K.; Brucher, R.; Russell, D. Cerebral emboli during left heart catheterization may cause acute brain injury. *Eur. Heart. J.* **2005**, *26*, 1269–1275. [[CrossRef](#)]
40. Skjelland, M.; Michelsen, A.; Brosstad, F.; Svennevig, J.L.; Brucher, R.; Russell, D. Solid cerebral microemboli and cerebrovascular symptoms in patients with prosthetic heart valves. *Stroke* **2008**, *39*, 1159–1164. [[CrossRef](#)]
41. Mitchell, S.J.; Benson, M.; Vadlamudi, L.; Miller, P. Cerebral arterial gas embolism by helium: An unusual case successfully treated with hyperbaric oxygen and lidocaine. *Ann. Emerg. Med.* **2000**, *35*, 300–303. [[CrossRef](#)]
42. Shah, A.S.; Akhmerov, A.; Gupta, N.; Chakravarty, T.; Makkar, R.R.; Azizzadeh, A. Use of a Dual-Filter Cerebral Embolic Protection Device in Thoracic Endovascular Aortic Repair. *Ann. Vasc Surg.* **2020**, *65*, 54.e1–54.e4. [[CrossRef](#)]
43. Van Gils, L.; Kroon, H.; Daemen, J.; Ren, C.; Maugenest, A.M.; Schipper, M.; De Jaegere, P.P.; Van Mieghem, N.M. Complete filter-based cerebral embolic protection with transcatheter aortic valve replacement. *Catheter. Cardiovasc. Interv.* **2018**, *91*, 790–797. [[CrossRef](#)]
44. Shimamura, K.; Kuratani, T.; Kin, K.; Shijo, T.; Masada, K.; Sawa, Y. Effectiveness of embolic protection filter devices in stroke prevention during endovascular aortic arch repair in significant aortic atheroma patients. *Interact. Cardiovasc. Thorac. Surg.* **2019**, *28*, 974–980. [[CrossRef](#)] [[PubMed](#)]
45. Tsutsumi, M.; Kazekawa, K.; Onizuka, M.; Kodama, T.; Nii, K.; Aikawa, H.; Iko, M.; Tomokiyo, M.; Matsubara, S.; Tanaka, A. Cerebral protection during retrograde carotid artery stenting for proximal carotid artery stenosis. *Neurol. Med. Chir.* **2007**, *47*, 285–288. [[CrossRef](#)] [[PubMed](#)]
46. Masada, K.; Kuratani, T.; Shimamura, K.; Kin, K.; Shijo, T.; Goto, T.; Sawa, Y. Silent cerebral infarction after thoracic endovascular aortic repair: A magnetic resonance imaging study. *Eur. J. Cardiothorac. Surg.* **2019**, *55*, 1071–1078. [[CrossRef](#)] [[PubMed](#)]
47. Ribo, M.; Molina, C.A.; Alvarez, B.; Rubiera, M.; Alvarez-Sabin, J.; Matas, M. Transcranial Doppler monitoring of transcervical carotid stenting with flow reversal protection: A novel carotid revascularization technique. *Stroke* **2006**, *37*, 2846–2849. [[CrossRef](#)]
48. Luk, Y.; Chan, Y.C.; Cheng, S.W. Transcarotid Artery Revascularization as a new Modality of Treatment for Carotid Stenosis. *Ann. Vasc. Surg.* **2020**, *64*, 397–404. [[CrossRef](#)]
49. Rippel, R.A.; Rolls, A.E.; Riga, C.V.; Hamady, M.; Cheshire, N.J.; Bicknell, C.D. The use of robotic endovascular catheters in the facilitation of transcatheter aortic valve implantation. *Eur. J. Cardiothorac. Surg.* **2014**, *45*, 836–841. [[CrossRef](#)]
50. Perera, A.H.; Riga, C.V.; Monzon, L.; Gibbs, R.G.; Bicknell, C.D.; Hamady, M. Robotic arch catheter placement reduces cerebral embolization during thoracic endovascular aortic repair (TEVAR). *Eur. J. Vasc. Endovasc. Surg.* **2017**, *53*, 362–369. [[CrossRef](#)]
51. Martens, S.; Neumann, K.; Sodemann, C.; Deschka, H.; Wimmer-Greinecker, G.; Moritz, A. Carbon dioxide field flooding reduces neurologic impairment after open heart surgery. *Ann. Thorac. Surg.* **2008**, *85*, 543–547. [[CrossRef](#)]
52. Listewnik, M.; Kotfis, K.; Ślózowski, P.; Mokrzycki, K.; Brykczyński, M. The influence of carbon dioxide field flooding in mitral valve operations with cardiopulmonary bypass on S100β level in blood plasma in the aging brain. *Clin. Interv. Aging.* **2018**, *25*, 1837–1845. [[CrossRef](#)]

53. Kalpokas, M.; Nixon, I.; Kluger, R.; Beilby, D.; Silbert, B. Carbon dioxide field flooding versus mechanical de-airing during open-heart surgery: A prospective randomized controlled trial. *Perfusion*. **2003**, *18*, 291–294. [[CrossRef](#)]
54. Kölbl, T.; Rohlf, F.; Wipper, S.; Carpenter, S.W.; Debus, E.S.; Tsilimparis, N. Carbon dioxide flushing technique to prevent cerebral arterial air embolism and stroke during TEVAR. *J. Endovasc. Ther.* **2016**, *23*, 393–395.
55. Hanna, L.; Perera, A.; Grover, G.; Singh, A.; Hamady, M.; Bicknell, C.B.; Gibbs, R. Carbon-Dioxide Flushing in Thoracic Aortic Stenting to Reduce Neurological Brain Injury: An observational case-control study. In Proceedings of the 68th International Congress 2019, European Society of Cardiovascular and Endovascular Surgery, Groningen, The Netherlands, 22–25 May 2019.
56. Rohlf, F.; Tsilimparis, N.; Trepte, C.; Kratzberg, J.; Mogensen, J.; Debus, E.S.; Kölbl, T. Air embolism during TEVAR: An additional flush port on the delivery system pusher significantly reduces the amount of air released during deployment of a thoracic stent-graft in an experimental setting. *J. Endovasc. Ther.* **2018**, *25*, 435–439. [[CrossRef](#)]
57. Rohlf, F.; Trepte, C.; Ivancev, K.; Tsilimparis, N.; Makaloski, V.; Debus, E.S.; Kölbl, T. Air embolism during TEVAR: Liquid Perfluorocarbon absorbs carbon dioxide in a combined flushing technique and decreases the amount of gas released from thoracic Stent-grafts during deployment in an experimental setting. *J. Endovasc. Ther.* **2019**, *26*, 76–80. [[CrossRef](#)]
58. Gerriets, T.; Schwarz, N.; Sammer, G.; Baehr, J.; Stolz, E.; Kaps, M.; Kloevekorn, W.P.; Bachmann, G.; Schönburg, M. Protecting the brain from gaseous and solid micro-emboli during coronary artery bypass grafting: A randomized controlled trial. *Eur. Heart. J.* **2010**, *31*, 360–368. [[CrossRef](#)]
59. Haiman, G.; Nazif, T.; Moses, J.W.; Ashkenazi, A.; Margolis, P.; Lansky, A.J. Reduction of Cerebral Emboli: In vitro Study with a Novel Cerebral Embolic Protection Device. *Med. Devices (Auckl)* **2020**, *13*, 67. [[CrossRef](#)]



© 2020 by the authors. Licensee MDPI, Basel, Switzerland. This article is an open access article distributed under the terms and conditions of the Creative Commons Attribution (CC BY) license (<http://creativecommons.org/licenses/by/4.0/>).